

# Dilatometric study of isothermal phase transformation in a C-Mn steel

J. M. PRADO, J. J. CATALAN, M. MARSAL

*Departamento Ciencia de Materiales e, Ingeniería Metalúrgica, Universidad Politécnica de Cataluña, Barcelona, Spain*

A dilatometric study of the isothermal phase transformations in a low-alloy carbon steel is presented. The results show a TTT diagram consisting of three C shaped curves corresponding respectively to allotriomorphic ferrite-pearlite, Widmanstätten ferrite-pearlite and bainite transformations. These three temperature intervals are even better marked in a plot of total dilatation against temperature. A representation of  $\log(\Delta l/l)$  against  $\log t$ , at each holding temperature, gives information about the transformations taking place. Hence, it is suggested that the bainitic reaction also occurs in two consecutive stages. Similarly to the other two transformations, ferrite formation in the initial stage is followed by the subsequent precipitation of cementite and further ferrite. It is concluded that the three transformations are of similar nature, controlled by carbon diffusion, the different C-curves being produced by changes either in the growth or nucleation mechanisms.

## 1. Introduction

In spite of its industrial importance and the extensive research work done, the mechanisms of phase transformation in steels are not yet well understood. Traditionally, these transformations have been studied in two cases namely, isothermal (TTT) and continuous cooling transformations (CCT). The latter because of its industrial relevance and the former because of its academic interest. The result of all this effort has been the elaboration of TTT and CCT diagrams for practically all types of steels [1], and consequently a better knowledge of how the different alloying elements influence these curves.

It is generally admitted that the TTT diagram, for a transformation in which there is no change in the mechanisms of nucleation and growth, is C-shaped. Therefore, alloys presenting TTT diagrams composed of several C-shaped parts must have a different mechanism either of nucleation or growth (or both) in each of them.

Steels possess different types of TTT diagrams depending on their chemical compositions. In the case of carbon steels they are formed by only one C-curve, while for low-alloy steels, mainly those alloyed with chromium and molybdenum, the existence of two C-curves is well established [2]. They are separated by a "bay" more or less marked depending on the content of alloying element. In high-alloy steels they reach complete separation. Generally, the high temperature C-curve is ascribed to the formation of allotriomorphic ferrite and pearlite, while the low temperature one is thought to correspond to the bainitic transformation. According to this point of view [3, 4], bainite and allotriomorphic ferrite are formed by different nucleation mechanisms. Carbon diffusion will be the controlling parameter for allotriomorphic fer-

rite nucleation, while supersaturated ferrite, formed by lattice shear, will be the initial nucleus of ferritic bainite. Carbon diffusion out of the nuclei will allow their posterior growth. Even Widmanstätten ferrite is claimed to be formed in a similar way [3]. A different point of view is held by other authors, who claim for the bainitic transformation a diffusion-controlled reaction mechanism, the growth of bainitic ferrite is thought to take place as a diffusion-controlled movement of ledges, while the "bay" between the two C-curves is attributed to a solute drag like effect [5-7].

In this work a dilatometric study of the isothermal phase transformations of a low-alloy carbon steel is presented. The objective of this investigation has been to make a contribution in the understanding of phase transformations in steels, with special emphasis on the bainitic reaction and "bay" formation.

## 2. Experimental procedure

A commercial steel, which chemical composition is shown in Table I, has been used in this investigation.

The study of the isothermal transformation kinetics has been carried out by means of high-speed dilatometry and scanning electron microscopy. The dilatometer used was a Sadamel 18AVRF-2. Dilatometric specimens were tubular in shape, 25 mm long, 4 mm diameter, with a wall thickness of 0.4 mm. In order to avoid oxidation or decarburization they were nickel or gold plated. Specimens were austenized at 870°C for 15 min and quenched to the different holding temperatures by means of a nitrogen jet automatically

TABLE I Chemical composition (wt %) of steel

C	Si	Mn	S	Cr	Ni
0.38	0.23	1.41	0.116	0.22	0.18

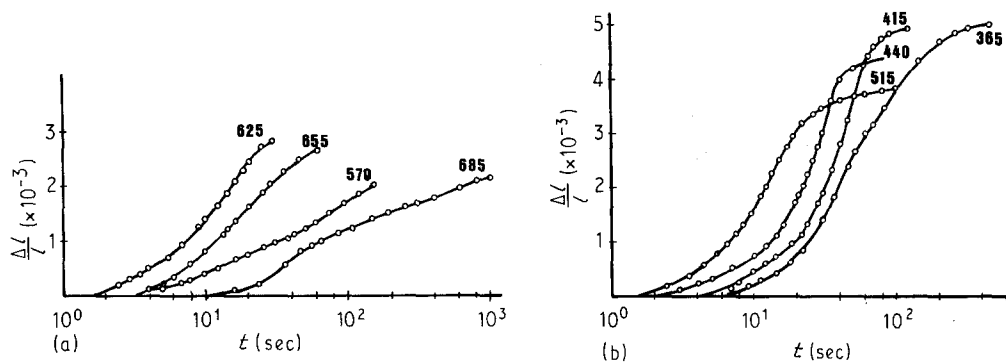


Figure 1 Variation of unit dilatation ( $\Delta l/l$ ) as a function of isothermal holding time.

controlled. In spite of this cooling technique, quenching velocities decreased with decreasing holding temperature, which made it impossible to study the isothermal transformation below a temperature of 360°C.

Samples for electron microscopy study were obtained from dilatometric specimens. They were manually polished, etched with nital and finally gold plated. The scanning electron microscope used was a Phillips PSEM-500.

Volume fractions of ferrite were determined by means of quantitative image analysis using a grid of 285 points.

### 3. Experimental results

#### 3.1. Dilatometry

Representative dilatometric results, covering the temperature interval under study, are shown in Fig. 1a and b. Curves obtained by means of the usual  $\Delta l/l$  against  $\log t$  plot, are of the sigmoidal type. The existence of two different and consecutive transformations, such as proeutectoid ferrite and pearlite, cannot be appreciated in them.

For this reason a less frequent kind of representation, namely  $\log \Delta l/l$  against  $\log t$ , was used. Fig. 2 illustrates the type of curves obtained when two different phases are formed. Curve (abce) corresponds to the case in which the second phase (ce) begins to form after the complete precipitation of the initial one (abc). Consequently a well marked discontinuity will appear in the curve. On the other hand, curve (abde)

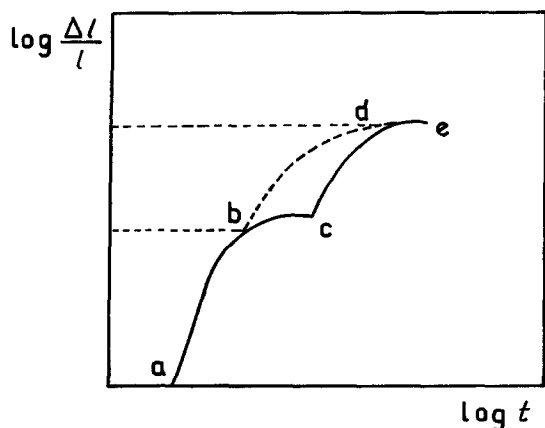


Figure 2 Schematic plot of  $\log \Delta l/l$  against  $\log t$  for the case of an isothermal transformation with two phases precipitating consecutively.

represents the case when the formation of one phase is initiated before the precipitation of the other has been completed. Now, and depending on the amount of overlapping, the discontinuity in the curve can be hardly visible.

In Fig. 3a, b and c dilatometric results are presented by means of this type of representation. Discontinuities in most of the curves, indicating the beginning of a second transformation, can now be seen. Nevertheless, curves corresponding to isothermal holdings of 655, 555 and 515°C do not show clearly this transition between the two stages of the global transformation, meaning that the onset of the pearlitic reaction takes place well before the completion of the ferritic one.

Dilatometric results corresponding to temperatures lying in the bainitic transformation interval (Fig. 3c)

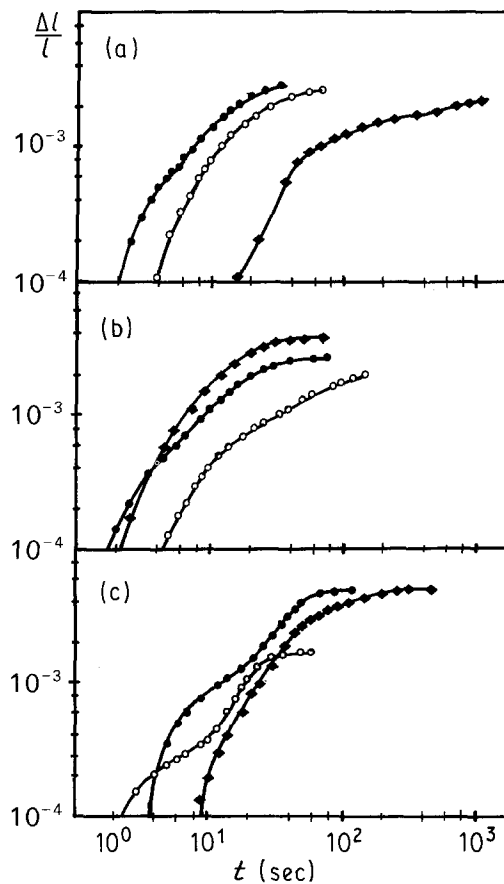


Figure 3 Dilatometric results of isothermal transformations plotted as  $\log \Delta l/l$  against  $\log t$ . (a) (●) 625°C; (○) 655°C; (◆) 690°C; (b) (●) 535°C; (○) 570°C; (◆) 515°C; (c) (●) 460°C; (○) 415°C; (◆) 370°C.

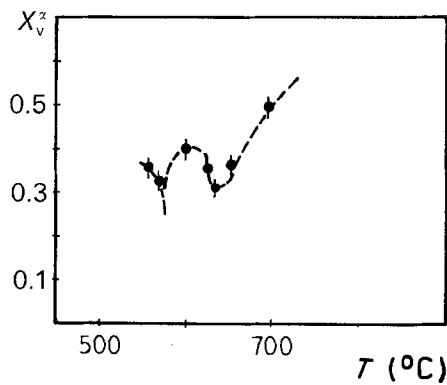


Figure 4 Variation of ferrite volume fraction ( $X_v^\alpha$ ) against temperature.

are of particular interest. A marked discontinuity exists in the curves implying that the bainitic reaction takes place also in two different stages as it has been previously suggested [8, 9].

Due to the overlap between the two stages of the isothermal transformation, it is not possible to assess directly from the dilatometric tests the values of the ferritic  $(\Delta l/l)_T^\alpha$  and pearlitic  $(\Delta l/l)_T^{\alpha+cm}$  total dilatations. However, they can be extrapolated if a linear relationship between  $(\Delta l/l)_T^\alpha$  and the ferrite content ( $X_v^\alpha$ ), what seems reasonable if the nucleation and growth mechanisms remain unchanged, is assumed. The value of  $(\Delta l/l)_T^\alpha$  given by Constant and Henry [10] for a 100% ferritic transformation has been used as the normalizing factor.

Fig. 4 shows the variation of proeutectoid ferrite volume fraction  $X_v^\alpha$ , determined by quantitative image analysis, with the temperature of isothermal holding. The value of  $X_v^\alpha$  has not been measured at temperatures below  $540^\circ\text{C}$  as it becomes increasingly difficult to distinguish between the ferrite formed in the first or second stage of the transformation. The ferrite content initially decreases reaching a minimum value at  $640^\circ\text{C}$ , from this temperature an increase in ferrite content occurs with a maximum at  $600^\circ\text{C}$ .

The variation of  $(\Delta l/l)_T^\alpha$  and  $(\Delta l/l)_T^{\alpha+cm}$  with the volume fraction of ferrite and pearlite respectively is shown in Fig. 5. Only isothermal holdings above

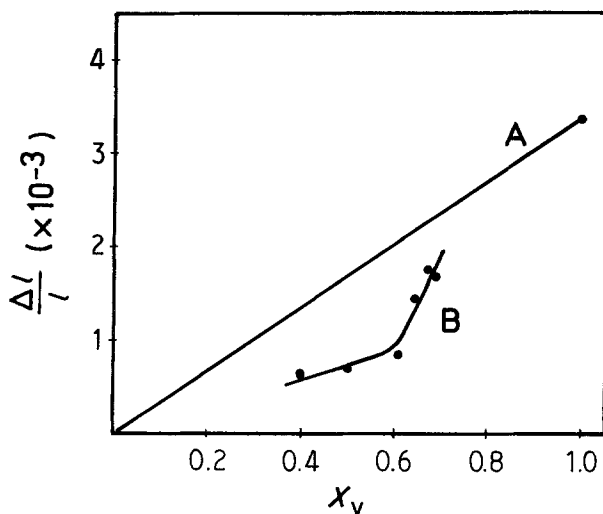


Figure 5 Variation of the unit dilatation of (A) ferrite and (B) pearlite precipitation as a function of ferrite and pearlite volume fractions respectively.

$570^\circ\text{C}$  are included in this figure, because below that temperature ferrite is of Widmanstätten type. The formation of acicular ferrite produces a dilatation due not only to the change of structure but also to the strain field of plate accommodation [3], therefore the linear relationship between  $(\Delta l/l)_T^\alpha$  and  $X_v^\alpha$  no longer holds. Pearlite dilatation,  $(\Delta l/l)_T^{\alpha+cm}$ , is smaller than that of ferrite (Fig. 5), but beyond certain volume fraction ( $\sim 0.6$ ) increases rapidly approaching the ferrite dilatation line. This behaviour can be understood considering that, for a fixed steel composition, the ferrite content of pearlite increases as the volume fraction of the latter phase also increases.

At temperatures below  $570^\circ\text{C}$  the values of  $(\Delta l/l)_T$  for the first and second stages of the transformation cannot be derived from Fig. 5. They have been determined directly from Fig. 3 when the discontinuity in the curve was well marked (small overlap between both transformations). When both transformations show a considerable overlap, the value of  $(\Delta l/l)_T$  for each one of them has been derived indirectly from the Johnson-Mehl-Avrami equation [11] in such a manner that the appropriate values of the exponent  $n$  are obtained. This aspect will be dealt with in more detail in a future article.

### 3.2. TTT curve

Fig. 6 shows the TTT curve obtained from the isothermal dilatometric tests. The curve includes together with the usual lines of beginning and end of transformation, a third line corresponding to the start of the second stage of the transformation, which can be of pearlitic or a degenerated type of this transformation occurring in low temperatures.

This curve presents a number of features which can be observed individually, but not simultaneously, in other TTT curves. At  $660^\circ\text{C}$  there is an inflection associated with the normal ferritic-pearlitic "nose". Around  $630^\circ\text{C}$  the curve shows an abrupt shift to the left. Aaronson and Domian [12] found a similar behaviour for a 3% Mn steel, it was initially attributed to the end of manganese partitioning during transformation but results obtained in this research [13] and

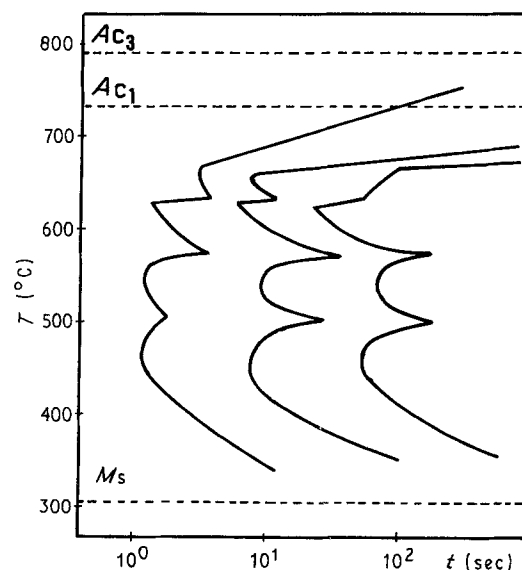


Figure 6 TTT curve derived from dilatometric results.

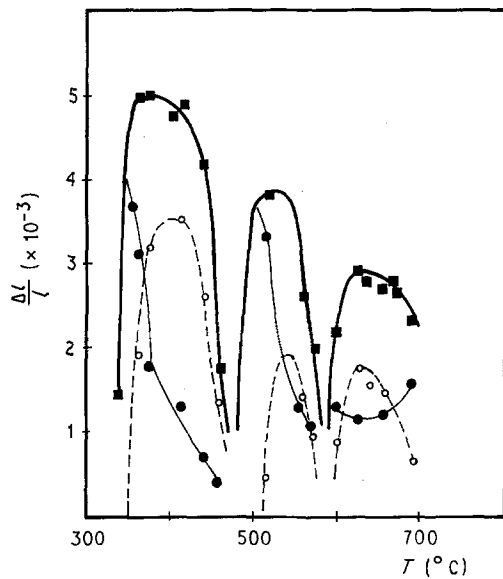


Figure 7 Variation of (■) total unit dilatation against temperature. (●) First and (○) second stages unit dilatations are also plotted.

those of Enomoto *et al.* [14] support a change from grain edge to grain surface boundary nucleation as the cause for the shift in the TTT curve.

A distinct “bay” occurs at 575 °C, similar to the one shown by medium and low alloyed steels, which is frequently identified as the bainitic bay. Results presented in this work and those of Bhadeshia [3] are in favour of considering this temperature as the one at which Widmanstätten ferrite starts to form.

Finally, another “bay” is hinted at around 500 °C, which corresponds to the one present in medium and high alloyed steels [1]. As it will be discussed later in this paper, this seems to be the true “bainitic bay”.

Most of these features are more clearly depicted in Fig. 7, which shows the variation of the total dilatation and that of the first  $(\Delta l/l)_T^{1st}$  and second  $(\Delta l/l)_T^{2nd}$  stages with the different temperatures of isothermal holding. The existence of three independent dilatation curves with deep minima between them is apparent. Each one of these curves is extended through temperature intervals which coincide with those defined in the TTT curve as corresponding to the allotriomor-

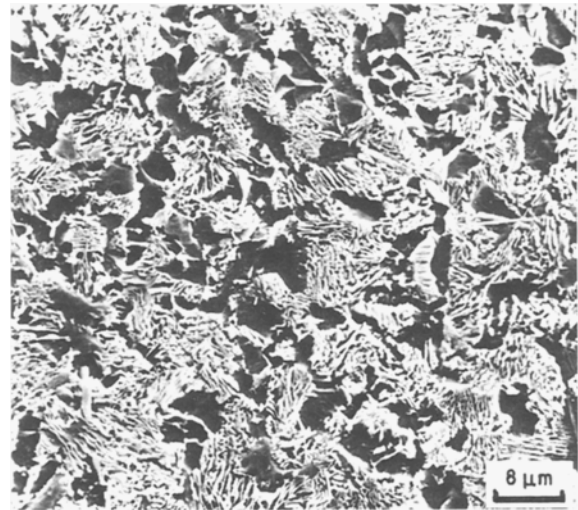


Figure 8 Microstructure of a full transformed specimen after an isothermal holding at 650 °C.

phic ferrite, Widmanstätten ferrite and bainite transformations. On the other hand, the abrupt shift in the TTT curve at 630 °C is now not present.

It is also interesting to observe the behaviour, in each of the three temperature intervals, of the curves corresponding to the first and second stages of the transformation. In all cases an inverted U-shaped curve is obtained for the variation of  $(\Delta l/l)_T^{2nd}$  with isothermal holding; while that of  $(\Delta l/l)_T^{1st}$  is U-shaped for  $T > 570$  °C and inverted U-shaped in the other two temperature intervals. The maximum and the minimum of the  $(\Delta l/l)_T^{2nd}$  and  $(\Delta l/l)_T^{1st}$  curves, for  $T > 570$  °C, occur at the same holding temperature. In the other two intervals the maxima of both curves are shifted apart, with the one of  $(\Delta l/l)_T^{2nd}$  occurring at the higher temperature end of the interval.

### 3.3. Microscopy

A microscopic examination shows clear microstructural differences between the three temperature intervals previously defined in the dilatometric tests. At temperatures above 570 °C the microstructure consists of allotriomorphic ferrite and pearlite, as it is shown in Fig. 8 for an isothermal holding at 650 °C. The main

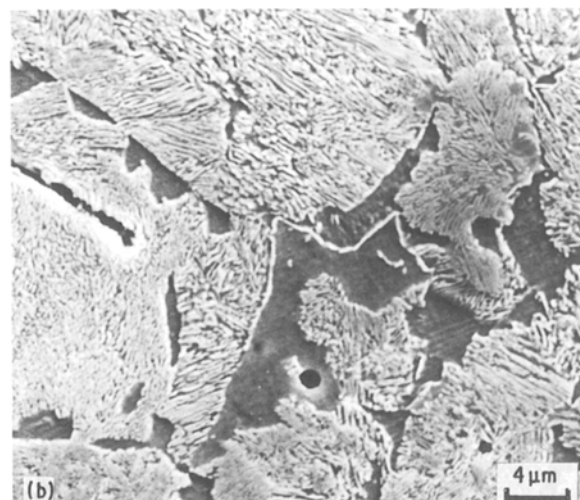
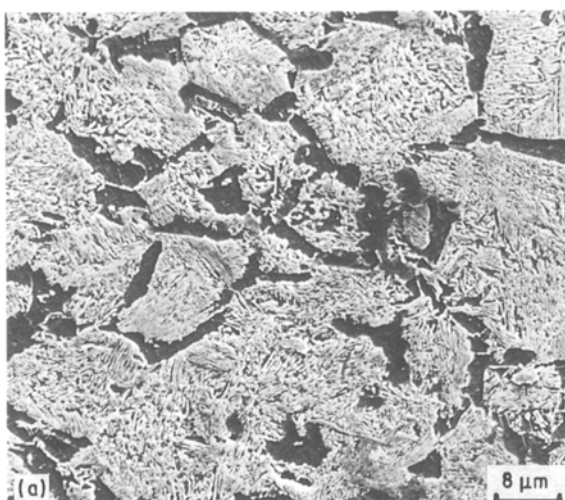


Figure 9 Microstructures of a specimen fully transformed at 570 °C. (a) General view; (b) detail showing ferrite side-plates.

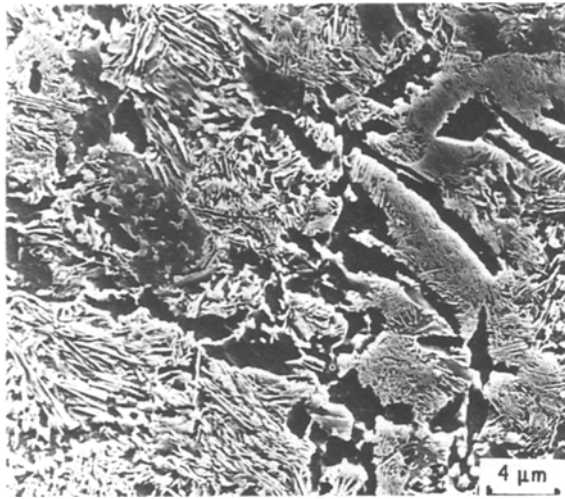


Figure 10 Microstructure of a specimen transformed at 550°C.

difference among the different temperatures being the volume fraction of each phase formed. Fig. 9a shows the microstructure obtained at 570°C, just below the first “bay” of the TTT curve. It is formed by ferrite and pearlite as in the case of temperatures above the bay; the main difference being the existence of ferrite side-plates growing from allotriomorphs and individual ferrite plates inside the grains (Fig. 9b). The occurrence of ferrite plates of Widmanstätten type is more clear at 550°C, their aspect ratio and number is now higher (Fig. 10). This trend is more marked at lower temperatures. Fig. 11a shows the microstructure formed at an isothermal holding at 515°C, the Widmanstätten plates are now separated by austenite–martensite islands. Well defined pearlitic areas are not visible, in good agreement with the small second stage dilatation occurring at this temperature (Fig. 7). This latter stage has only just been initiated before the transformation is halted. This phenomenon is known as “incomplete reaction” [4, 15] and it is not yet well understood, Fig. 11b illustrates the way in which the second stage of the transformation takes place, it shows two different types of “untransformed

islands”, one of them is quite featureless and corresponds to a martensite transformed, during posterior cooling, carbon enriched austenite area. In the other one, rows of cementite have already been precipitated, but the transformation has not proceeded further, Fig. 12 shows the microstructure obtained after an isothermal holding at 470°C. This temperature lies just below the “bainitic bay” and according to Fig. 7 only a small dilatation, most of it deriving from second stage, occurs. The “incomplete reaction” can be appreciated by the remaining number of “untransformed islands” all of them showing the cementite precipitation. At 415°C the transformation is carried out more thoroughly, but again due mainly to the second stage of the bainite reaction. The very fine structure obtained at this temperature is shown in Fig. 13. Only a few “untransformed islands” can now be seen. At 370°C the first stage of the bainitic reaction becomes preponderant, while the second stage decreases. Bainitic ferrite plates, formed at that temperature during the first stage and separated by cementite, can be seen in Fig. 14. It also shows the presence of untransformed areas with cementite precipitated inside them.

It is patent, from the micrographs shown, that a great difficulty exists in distinguishing between the microconstituents formed during the first and the second stages of the bainitic transformation.

#### 4. Discussion

As it has been indicated this steel presents three types of well differentiated transformations, which show in the TTT curve and are particularly noticeable in the  $(\Delta l/l)_T-T$  curve (Fig. 7). They are:

1. “Ferritic–pearlitic” transformation. It takes place at temperatures above 570°C. Allotriomorphic ferrite and laminar pearlite are its final products.
2. “Widmanstätten ferrite–pearlite” transformation. It occurs between 570 and 500°C. Ferrite precipitates become more plate-like as holding temperature decreases. At the lower end of that temperature interval the pearlitic reaction is practically suppressed.

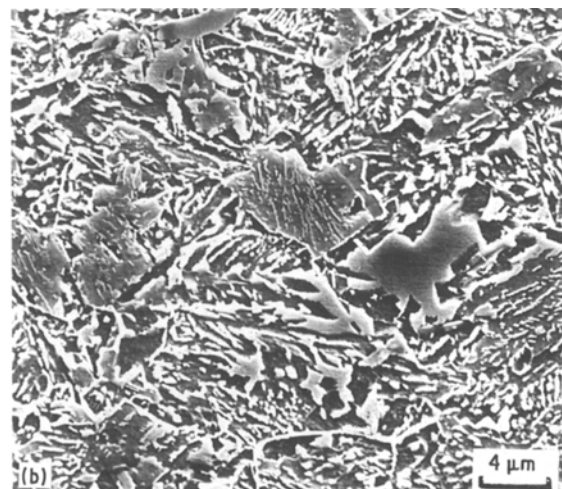
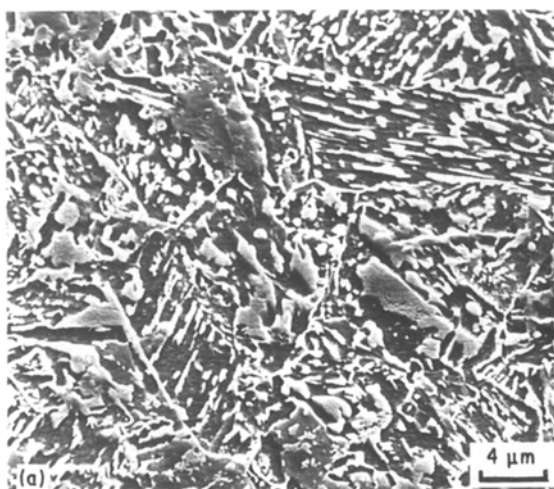


Figure 11 (a) Microstructure of a specimen transformed at 515°C; (b) same specimen showing the existence of “untransformed islands”.

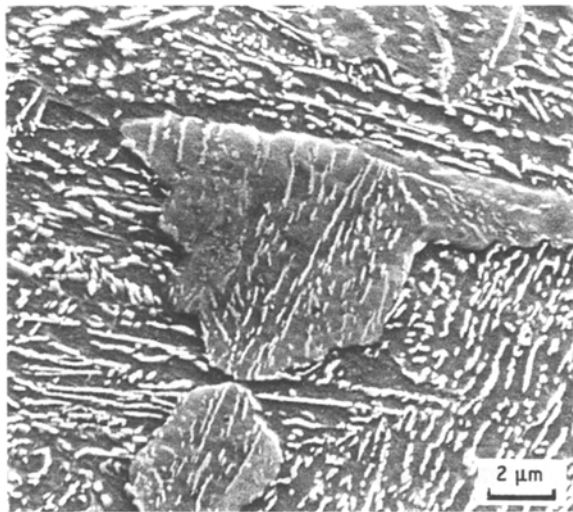


Figure 12 Microstructure of a specimen transformed at 470° C.

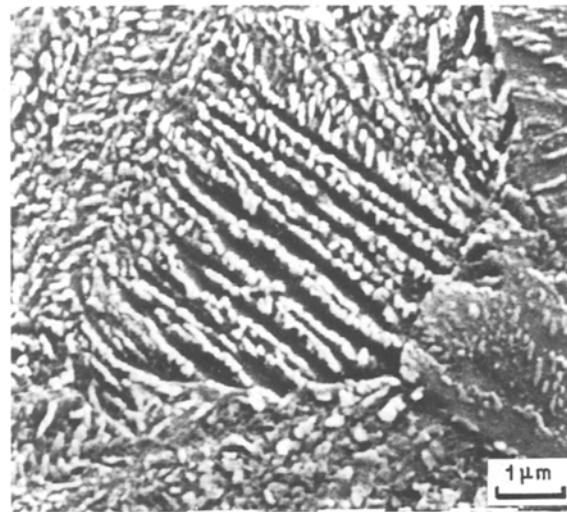


Figure 14 Microstructure of a specimen transformed at 370° C.

3. “Upper bainite” transformation. It takes place at temperatures below 490° C (and above  $M_s$ ), and similarly to the other two transformations, consists also of two different stages. At the upper end of the temperature interval the second stage of the transformation is predominant but it is again suppressed at the lower end.

Fig. 7 seems to indicate the possible existence of a fourth type of transformation between 350° C and  $M_s$ , which is thought to correspond with lower bainite. This temperature interval was not studied due to experimental difficulties.

The three transformations are separated by “bays”, that, in other terms, means that each one has its own C curve. Therefore, either the mechanism of nucleation or growth (or both) should change across each bay.

The variation in ferrite morphology from one side of the bay at 570° C to the other is evidently related to a change in the kinetics of transformation. Above 570° C ferrite grows as allotriomorphs, below that temperature it becomes gradually more Widmanstätten-like (Figs 8–11). It is now well established that the interface between ferrite allotriomorphs and austenite is formed by ordered and disordered areas [16–18]. Hence, it is reasonable to suppose that above

570° C ferrite growth is mainly due to the advance of ordered interfaces by the lateral motion of ledges, while disordered ones migrate at lower rates. Below 570° C the situation can be inverted, disordered interfaces become progressively more mobile while the migration rate of ordered areas decreases continuously with undercooling. This picture is in good agreement with the solute drag-like effect proposed by Aaronson and co-workers [6, 19, 20]. Segregation of manganese and chromium to the disordered areas of the ferrite– austenite interfaces will slow down their migration rates. If below 570° C this segregation decreases the development of ferrite Widmanstätten structure will be reached. The overall effect will be the occurrence of a bay at the TTT diagram. Hence, the continuous variation of microstructure across the bay will favour a change in the growth for the slow-down of the transformation kinetics at 570° C. Therefore, a change into shear nucleation mechanism, as it has been proposed by Bhadeshia [3], does not seem necessary in order to explain the experimental results obtained at that temperature.

The commercial steel used in this work contains manganese as its main alloying element and chromium only as residual one. However, the TTT diagram obtained combines aspects common to steels alloyed with each one of these elements. The abrupt shift to the left at 620° C seems characteristic of manganese alloyed steels, but they do not show the bay at 570° C [12, 14], which, on the other hand, is present in steels alloyed with chromium [12, 21]. This latter element produces the solute drag-like effect more effectively than manganese [20]. Hence, it is probably the chromium content, enhanced by manganese, that is responsible for the change in growth mechanism, and consequently for the bay, at 570° C.

As it has been indicated the ferrite morphology becomes more Widmanstätten-like as temperature decreases. At 515° C (Fig. 11) it is difficult to appreciate the existence of allotriomorphs of ferrite. The pearlitic reaction takes place at the higher temperature end, practically to completion. At lower temperatures the rapid growth of ferrite plates enriches the

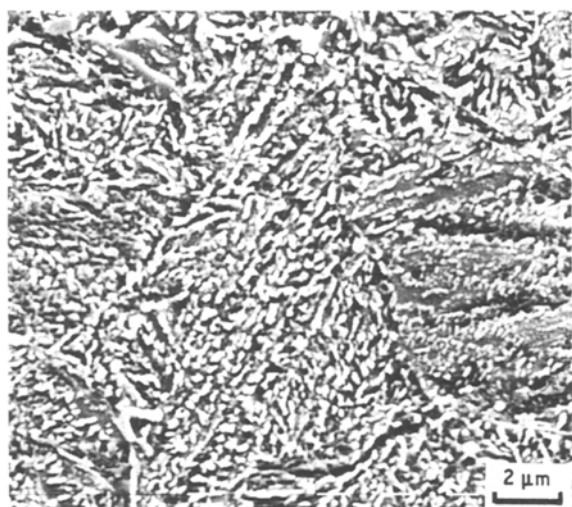


Figure 13 Microstructure of a specimen transformed at 415° C.

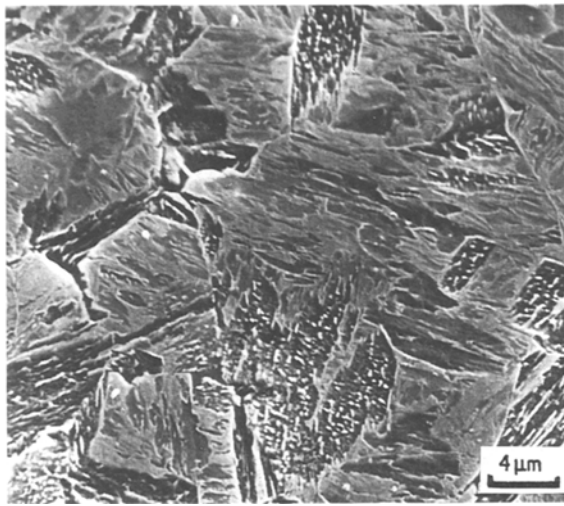


Figure 15 Microstructure of a specimen held for 7 sec at 380°C.

untransformed austenite with carbon to such a degree that the pearlitic transformation stops, giving place to what is known as “incomplete reaction” (Fig. 11).

The existence of a bay at 490°C is hardly perceptible in the TTT diagram, but it is remarkably well defined in the plot of  $(\Delta l/l)_T$  against temperature (Fig. 7). According to this graph transformation reaches an “extasis” and starts again at lower temperatures, which seems to indicate that a new change in the mechanism of transformation has taken place. In a previous paper [22] experimental evidence for the change in the mechanism of nucleation has been presented. It is proposed that during the incubation period carbon diffusion occurs, leaving areas of austenite enriched and depleted with carbon.

Ferrite nucleation takes place in the carbon depleted areas, because the thermodynamic drive for transformation will be higher in them. This kind of behaviour is illustrated in Fig. 15 which shows the microstructure of a specimen held isothermally at 380°C for 7 sec. Plain dark grey plates, together with other ones where further transformation has occurred can be seen. They correspond to the carbon depleted austenite areas where ferrite is nucleated. Transformation is carried out by repeated nucleation of ferrite subunits inside those plates. The mechanism is in a way the opposite to the one proposed by other authors [3, 4], namely nucleation of supersaturated ferrite with posterior diffusion of the carbon.

According to Figs 3 and 7 the bainitic transformation consists also of two stages. In the first one, mainly ferrite is formed by the above exposed mechanism. Carbides can also precipitate in those areas, near or between ferrite plates, with the right amount of carbon. But the basic feature of this stage is the long distance diffusion of carbon and consequently the enrichment of the untransformed austenite with this element.

The second stage starts once the carbon depleted areas are fully transformed. Carbide precipitation in the remaining austenite promotes the nucleation of ferrite, but the characteristic feature of this stage is that carbon diffuses only over short distance. Fig. 16 corresponds to a specimen held isothermally at 490°C

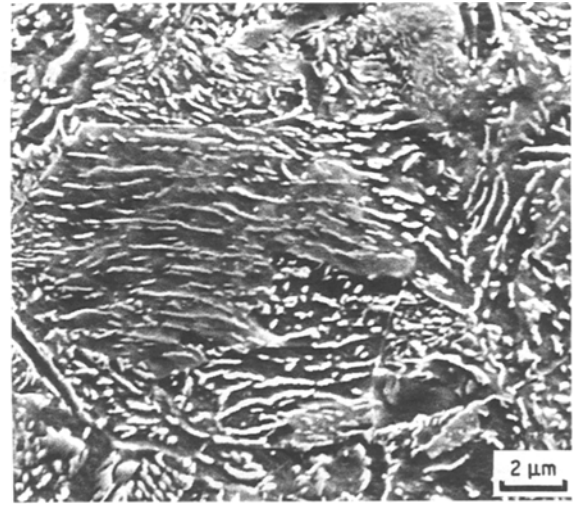


Figure 16 Microstructure of a specimen transformed at 490°C.

after the transformation has stopped, therefore the second stage was in operation, and it shows a partially transformed area. The right hand corner is already transformed but in the rest transformation is not yet completed. The precipitation of carbide rows, lowering the carbon content of the austenitic matrix seems to be the initial step of this second stage of the transformation. A similar behaviour has also been shown to occur in specimens just above the bainitic bay (Fig. 11b).

The existence of two stages in the bainitic transformation is well established in silicon alloyed steels [8, 9] and in austempered ductile iron [23, 24]. In both cases the presence of silicon retards the formation of carbides making easier to recognize microstructurally the two stages. The present work proves that it is also common to low-alloy hypoeutectoid steels. In a future article the Johnson–Mehl–Avrami equation will be used to study in more detail these two stages.

It is now interesting to examine the dilatation results represented in Fig. 7. The value of the three maxima, corresponding to the total unit dilatation for the temperature intervals of allotriomorphic, Widmanstätten and bainitic ferrite transformations, increases with decreasing temperature, reflecting the effect of the strain field for plate accommodation. The maxima for the bainitic and Widmanstätten ferrite unit dilatation are very alike meaning probably that the nature of both constituents is similar. Also, pearlitic dilatation both above and below the Widmanstätten bay are of the same magnitude which, together with no variation in the microstructural aspect, is a clear indication that the mechanism of the pearlitic reaction does not change across the bay. In the bainitic second stage unit dilatation reaches a maximum markedly higher than those of pearlite in the other two temperature intervals. Also, the microstructural aspect of both constituents are very dissimilar. Hence, the mechanisms involved in both transformations, pearlite and bainitic second stage, should be of a different nature. Probably the main difference between the first and second stages is the way in which carbon diffusion controls the transformation.

## 5. Conclusions

The dilatometric study of this steel shows the existence of three types of transformations. Their temperature intervals of existence are reflected in the TTT diagram, but are particularly well defined in the  $(\Delta l/l)_T$  against  $T$  plot. They are:

1. Allotriomorphic ferrite-pearlite, above 570°C.
2. Widmanstätten ferrite-pearlite, between 570 and 490°C.
3. Upper bainite, between 490 and 350°C.

These transformations are separated by "bays" in both diagrams. The occurrence of the first bay at 570°C is explained as a consequence of the solute drag-like effect, which allows for a change in the growth mechanism of proeutectoid ferrite. The bay at 490°C is justified through a change in the nucleation mechanism. Carbon diffusion during the incubation period creates austenite areas rich and poor in carbon content. Ferrite nucleation is enhanced in the latter ones.

Dilatometry and microscopy also show the existence of two distinct stages in the bainitic transformation. In the first stage ferrite is formed (some cementite can also be formed as a secondary product) and its growth is controlled by carbon diffusion over long distances. Cementite is initially precipitated in the second stage, followed by ferrite nucleation. Short distance carbon diffusion is now the controlling factor of the transformation.

## References

1. "Atlas zur Wärmebehandlung der Stähle", (Verlag Stahleisen M.B.H. Düsseldorf, 1961).
2. N. F. KENNON, *Met. Trans.* **9A** (1978) 57.
3. H. K. D. H. BHADASHIA, *Acta Metall.* **29** (1981) 1117.
4. H. K. D. H. BHADASHIA and D. V. EDMONDS, *Acta Metall.* **28** (1980) 1265.
5. R. F. HEHEMANN, K. R. KINSMAN and H. I. AARONSON, *Met. Trans.* **3** (1972) 1077.
6. H. I. AARONSON, S. K. LIU, W. T. REYNOLDS JR and G. J. SHIFLET, *J. Mater. Sci.* **20** (1985) 4232.
7. H. I. AARONSON, J. M. RIGSBEE and R. K. TRIVERDI *Scripta Met.* **20** (1986) 1299.
8. B. P. J. SANDVIK, *Met. Trans.* **13A** (1982) 777.
9. *Idem, ibid.* **13A** (1982) 789.
10. A. CONSTANT and G. HENRY, *Trait. Thermique* **155** (1981) 47.
11. J. W. CHRISTIAN, "Transformation in Metals and Alloys" Part I, (Pergamon, Oxford, 1975) p. 525.
12. H. I. AARONSON and H. A. DOMIAN, *Trans. TMS-AIME* **236** (1966) 781.
13. J. M. PRADO, unpublished results (1986).
14. M. ENOMOTO, W. F. LANGE and H. I. AARONSON, *Met. Trans.* **17A** (1986) 1399.
15. H. K. D. H. BHADASHIA and D. V. EDMONDS, *ibid.* **10A** (1979) 895.
16. J. R. BRADLEY, J. M. RIGSBEE and H. I. AARONSON, *ibid.* **8A** (1977) 323.
17. G. R. PURDY, *Acta Metall.* **26** (1978) 477.
18. *Idem, ibid.* **26** (1978) 487.
19. S. K. LIU, W. T. REYNOLDS JR, H. HU, G. J. SHIFLET and H. I. AARONSON, *Met. Trans.* **16A** (1985) 457.
20. J. R. BRADLEY and H. I. AARONSON, *ibid.* **12A** (1981) 1729.
21. G. J. SHIFLET, H. I. AARONSON and J. R. BRADLEY *ibid.* **12A** (1981) 1743.
22. J. M. PRADO, *J. Mater. Sci. Lett.* **5** (1986) 1075.
23. J. F. JANOWAK and R. B. GUNDLACK, *AFS Transactions* **54** (1983) 377.
24. Y. J. PARK, P. A. MORTON, M. GAGNE and R. GALLER, *ibid.* **153** (1984) 395.

Received 17 May  
and accepted 29 June 1989